MULTI-SCALE SPOT SEGMENTATION WITH SELECTION OF IMAGE SCALES

Bertha Mayela Toledo Acosta[⋆] *Antoine Basset*[⋆†] *Patrick Bouthemy*[⋆] *Charles Kervrann*[⋆]

[⋆]Inria, Centre Rennes - Bretagne Atlantique, France
[†]CNES, Toulouse, France

ABSTRACT

Detecting spot-like objects of different sizes in images is needed in many applications. Multiple image scales must then be handled for reliable spot segmentation. We define an original criterion based on the *a contrario* approach and the LoG scale-space framework to automatically select the meaningful scales. We then design a coarse-to-fine multi-scale spot segmentation scheme involving a locally adaptive thresholding across scales, to come up with the final map of segmented spots. We report experimental results on simulated and real images of different types, and we demonstrate that our method outperforms other existing methods.

***Index Terms*—** Multi-scale spot detection, automatic scale selection, *a contrario* approach, object segmentation

1. INTRODUCTION

In many cases, image content may consist of a collection of elements, such as cars in traffic monitoring, boats on the ocean in remote sensing, stars in astronomy, animals in observation of natural scenes, cells and subcellular elements in microscopy imaging, to name a few. If they are small enough or seen from a distance, they usually appear as similar spots of a more or less regular shape. Thus, detecting spots in images is a common prerequesite in many applications. In order to countervail noise resulting from the image acquisition stage or the presence of spurious elements, selecting the right image scale is needed to correctly detect spots of interest. For a given scale, a spot detection framework can be divided in three sub-steps : first, image preprocessing to smooth out noise; second, signal enhancement to highlight spots to detect; third, spot detection by thresholding; the two first ones being often merged in a single operator.

However, elements of interest may not all correspond to the same image scale, if the collection includes subgroups of different sizes or if perspective effects occur. Then, the need is not merely the selection of the optimal scale, but of all the meaningful scales. We will deal with the problem of multi-scale spot detection with an automated selection of the meaningful scales. Our primary interest is to detect particles in microscopy images, but our method can be applied to other types of images as well. Our method adopts the *a contrario* approach for multi-scale selection, and performs locally adaptive thresholding across scales for spot segmentation.

The remainder of the paper will be organized as follows. In Section 2, we will provide a brief review of spot detection methods. Section 3 will be devoted to the presentation of our multi-scale spot detection method. In Section 4, we will report experimental results on simulated data with an objective comparative evaluation, and on real images of various kinds. Finally, Section 5 will contain concluding remarks.

2. RELATED WORK

Many efforts have been made towards automatic spot detection in images. More detailed information on existing methods along with experimental comparative evaluation of several spot detection methods can be found in [1, 2, 3]. Methods can be divided in single-scale and multi-scale approaches.

Single-scale methods [4, 5, 6] extract spots from an image, corresponding to one given size. The scale parameter is usually predefined. In [6] and [7], a mixture of Gaussian models is used to detect overlapping spots, while approaches based on the top-hat scheme are used in [8] and [9]. Methods based on *h*-dome [10, 11, 12] can deal with close particles by detecting domes or local intensity maxima. In [5], a single-scale spot-enhancing filter (SEF) is presented, where the Laplacian of Gaussian (LoG) filter is used to detect spots in fluorescence microscopy images. The LoG filter enhances structures of a determined size, corresponding to the variance of the Gaussian filter involved, while smoothing the image, and removing (to a certain extent) background structures.

However, the standard deviation of the Gaussian filter within the LoG transform needs to be adapted to the size of the particles to detect. We introduced a statistical criterion in [3] to automatically select one single optimal scale, based on the scale-space paradigm of [13] and a discrete version of the Gaussian filter. The selected scale is the one corresponding to the maximum number of blobs normalized by the number of blobs in a pure noise image at the same scale, where blobs designate local extrema in the scale-space domain.The resulting spot detection method was proven to outperform existing methods on several benchmarks. It was applied to

This work has been partly supported by the National Council of Science and Technology of Mexico (CONACYT) under the Grant no. 246372/384571.

vesicle segmentation in total internal reflection fluorescence microscopy (TIRFM) images [3].

Multiscale methods are able to extract spots of different sizes from an image. In [14] a general Gaussian scale-space framework was investigated to select multiple scales for blob and junction detection. [15] locally selects the most salient scale for region contour points to drive the PDE-based image segmentation. In [16] a non-linear scale-space representation employing a differential morphological decomposition, is used for multiscale corner detection. In [17], an isotropic undecimated wavelet method is designed to detect biological particles of different sizes, exploiting the wavelet multiscale product introduced in [18]. In [19], a generalized Laplacian of Gaussian allows to detect circular and elongated structures, while estimating their dimensions and orientations. In [20], a multiscale spot detection scheme, exploiting the LoG transform, is developed and used together with a multi-frame association algorithm to track virus particles. Multi-scale LoG scheme was also adopted for pulmonary nodule detection in [21], with 150 predefined LoG kernels of incrementally increasing sizes.

We propose a new multi-scale spot detection method based on the LoG transform, able to automatically select the meaningful scales in the processed image. Moreover, we will design a locally adaptive thresholding process across scales to come up with the final map of segmented spots.

3. MULTISCALE SPOT DETECTION

In this section, we present our multiscale spot detection method. It is divided in two main stages: the multi-scale selection step, where we recover the meaningful scales corresponding to the significant objects in the image, and the detection step, where we exploit the selected scales to compose the binary map of segmented spots of different sizes. For both stages, we will rely on the LoG transform as we did in [3]. However, in [3], we dealt with a single scale paradigm. To select multiple scales, we introduce a new criterion based on the *a contrario* approach. The detection step is also modified to combine the LoG output obtained at different scales.

3.1. A contrario selection of multiple scales

We rely on the *a contrario* approach [22], to select the meaningful scales. Briefly speaking, the *a contrario* approach can be viewed as a hypotheses test, where only the null hypothesis H_0 needs to be specified, which is called the background model accounting for randomness. A structured element is likely to appear under H_0 only with a very low probability. This approach was successful for several pattern detection problems. It was also investigated for motion detection [23]. To our knowledge, it is applied to scale selection for the first time. In [24], it was explored to predict the detectability of spots in textured images.

Let us consider an image f over the domain Ω, containing spots of various sizes and corrupted by Gaussian noise. The issue is how to automatically select the meaningful scales. We start from a set of scales $\mathcal{S} \subset \mathbf{R}_+^*$, as in [3], defined by $\mathcal{S} = \{s_0 r^n, n \in [0, \nu]\}$, where s_0 is taken equal to 1, r is close to 1 (e.g., 1.2), and ν depends on the range of possible scales in the given application. Given $\mathcal{S}$, we build a scale-space representation of the image following [13], with a LoG transform based on a discrete analogous of the Gaussian filter to handle arbitrary scale values (let us remind that scale corresponds to the Gaussian variance, and spot radius to the standard deviation). We come up with a 3-dimension map H_f, where each slice corresponds to the LoG filtered image for a given scale $s \in \mathcal{S}$:

$$\forall (p,s) \in \Omega \times \mathcal{S}, H_f(p,s) = (K_s * f)(p,s), \qquad (1)$$

where K_s denotes the LoG kernel of variance s. The response of a bright spot of size ς and located at point p, to the multiscale LoG transform should be minimum at $p \in \Omega$ and scale $s \in \mathcal{S}$, where s is the closest value to ς^2. Such a scale-space minimum is named *blob*, following [13].

To detect spots as reliably as possible, we need to find the scales at which LoG best enhances them, while reducing noise. To do so, we elaborate a probability measure to account for the ability of the LoG to distinguish noise and spots. We have no prior information on the spots, but we suppose that the noise is Gaussian. Thus, we construct a model representing the situation where no spots are present (H_0 hypothesis), that is, an image containing only uncorrelated Gaussan noise. Then, we denote by N_s the random variable representing the number of blobs at scale s in such a random image.

We can assume that the probability for any point $p \in \Omega$ to be a blob at scale s follows a binominal distribution of mean μ_s. Then, the variable N_s of the number of blobs at scale s is Poisson-distributed of mean $\lambda_s = \mu_s |\Omega|$, where $|.|$ denotes the cardinality of the set. Let $\mathcal{G} = \{g_i, 1 \leq i \leq M\}$ be a set of M such random images, and let $n_s(g_i)$ be the computed number of blobs in g_i at scale s. We showed in [3] that $n_s(g_i)$ is unchanged when adding any constant to g_i or multiplying g_i by any positive number. Therefore, we merely consider a normalized Gaussian noise, $\forall p \in \Omega, g_i(p) \sim \mathcal{N}(0,1)$. We empirically estimate λ_s as the average number of blobs at scale s in the set $\mathcal{G}$ of M noise image samples:

$$\hat{\lambda}_s = \frac{1}{M} \sum_{i=1}^{M} n_s(g_i). \qquad (2)$$

Meaningful scales in image f will be those for which the number of blobs in H_f is the least likely to be high under the "no-spot" H_0 hypothesis, hence, the name of *a contrario* approach (it cannot happen "by chance"). To do so, we count the number $n_s(f)$ of blobs in H_f at every scale $s \in \mathcal{S}$, and we evaluate the probability that so many blobs may exist under the "no-spot" H_0 hypothesis. We refer to it as the probability of false alarm $\mathrm{PFA}(s, f)$, which can be estimated as:

$$\begin{aligned}\mathrm{PFA}(s,f) &= \mathbb{P}(N_s \geq n_s(f)) \\ &= 1-\Phi_{\lambda_s}(n_s(f)) \approx 1-\Phi_{\hat{\lambda}_s}(n_s(f)) \quad (3)\end{aligned}$$

where $\Phi_{\hat{\lambda}_s}$ is the cumulative density function (CDF) of the Poisson distribution of mean $\hat{\lambda}_s$:

$$\Phi_{\hat{\lambda}_s} = e^{-\hat{\lambda}_s} \sum_{i=0}^{n_s(f)} \frac{\hat{\lambda}_s^i}{i!}. \quad (4)$$

We come up with a set of probabilities $\{\mathrm{PFA}(s,f), s \in \mathcal{S}\}$, and we can simply select the subset of ϵ-meaningful scales $\mathcal{S}^\star \subset \mathcal{S}$ as given by:

$$\mathcal{S}^\star = \{s \in \mathcal{S} | \mathrm{PFA}(s,f) < \epsilon\}. \quad (5)$$

Let denote $|\mathcal{S}^\star| = \eta$. In practice, since we look for very low $\mathrm{PFA}(s,f)$, we arbitrarily fix ϵ to 0.1. Alternatively, in case we know *a priori* the number η of relevant spot sizes, we can select the scales corresponding to the η lowest PFAs.

3.2. Spot detection at a given scale

Once the set of scales $\mathcal{S}^\star$ is determined, we can build a spot detection binary map $\Delta_s : \Omega \to \{0,1\}$ for each scale $s \in \mathcal{S}^\star$. We will again exploit the LoG transform, since it smooths noise while enhancing spots. This will be achieved by thresholding the lowest (resp. highest) values of the corresponding LoG map $H_f(\cdot, s)$, $s \in \mathcal{S}^\star$, if spots are bright (resp. dark) in the image. We will automatically inferred the threshold value τ_s which will be adapted for every point $p \in \Omega$ from local statistics of the LoG map $H_f(\cdot, s)$ in the vicinity of p. It can be assumed that the local background in the LoG map is smooth and corrupted by a white Gaussian noise [3]. For every point $p \in \Omega$, we estimate the local mean $\mu_s(p)$ and variance $\sigma_s^2(p)$ over a Gaussian window $W_s(p)$. The likelihood $\mathcal{L}_s$ of belonging to the background of the LoG map in the vicinity of p at scale $s \in \mathcal{S}^\star$ is then defined by:

$$\mathcal{L}(p) = \varphi\left(\frac{H_f(p,s) - \mu_s(p)}{\sigma_s(p)}\right), \quad (6)$$

where φ denotes the density function of the standard normal distribution. Given a *p*-value α, the local threshold value is then inferred as $\tau_s(p) = \sigma_s(p)\varphi^{-1}(\alpha) + \mu_s(p)$. A point p is detected as belonging to a (bright) spot if $H_f(p,s) < \tau_s(p)$. α can be independently fixed for the experiment according to the reliability which is required or expected, while thresholding automatically adapts to local image statistics.

3.3. Multiscale spot detection

When detecting spots of different sizes, it is important to correctly combine results of spot segmentation obtained at different scales. Similarly to [20], we adopt a coarse-to-fine nested approach. The scheme is defined as follows. Let us consider the input image f and the set $\mathcal{S}^\star$ of the η meaningful scales selected at the first stage of our method, $\mathcal{S}^\star = \{s_l, l = 1, \eta\}$, ranked in decreasing order. At each scale $s_l \in \mathcal{S}^\star$, we compute the filtered image $\psi(p, s_l)$ given by:

$$\psi(p, s_l) = H_f(p, s_l)\Delta_{s_{l-1}}(p) \quad (7)$$

where $\Delta_{s_{l-1}}(p)$ is the spot detection binary map computed at scale s_{l-1}. For $l = 1$, corresponding to the coarsest scale or level, by definition we take $\Delta_{s_0}(p) = 1, \forall p \in \Omega$. The spot detection binary map at a given scale operates as a mask for spot detection at the subsequent finer scale. Indeed, this way, spurious spot detections are avoided at coarser scales, while at finer scales spots in close proximity can be further resolved. The spot segmentation map will be given by Δ_{s_η}. Thus, we compute the multi-scale spot detection map for several scales automatically selected on the processed image f, and there is just one single user-friendly parameter to set for the segmentation step, that is, the *p*-value α.

In contrast, the max, min and number of scales (for a regular scale sampling) have to be predefined by the user in [20], along with parameters in the thresholding and masking operations. This is also the case for [17], where the user has to set the threshold, max and min scales and the false discovery rate. In addition, we have implemented a variant, denoted AS-MSSEF, combining the coarse-to-fine spot detection framework of [20] with our automated scale selection.

4. EXPERIMENTAL RESULTS

We have evaluated the performance of our method on both synthetic and real images. We set the *p*-value to $\alpha = 0.001$ in all the experiments. We have compared our multiscale method with other multiscale methods: MSSEF [20], MS-VST [17], and the variant AS-MSSEF.

4.1. Simulated data

We generated two sets of 20 simulated images each. 150 Gaussian spots, of three equally distributed sizes ς (resp. for the two sets $\{\sqrt{2.6}, 2, \sqrt{6}\}$, and $\{\sqrt{3}, \sqrt{5}, \sqrt{7}\}$), were randomly sampled in each simulated image over a uniform zero-valued background. We added Gaussian noise to the image, of mean 2 and standard deviation 0.6, knowing that the spot peak intensity value is 10. The objective evaluation is divided in three steps: multiple scale selection, spot detection (spot center location), and spot segmentation. For the two last steps, we compare our method to the three other methods.

To assess multi-scale selection, we compute precision and recall scores. 100% recall means that all the true scales are correctly selected. 100% precision means that all the selected scales correspond to true scales. Since we start with a set of 18 predefined scales $\mathcal{S} = \{1, 1.2, 1.44, ..., 18.49, 22.19\}$, a true scale is stated as recovered if the scale the closest to it is selected among the tested ones. In the first experiment, precision amounts to 100% and recall to 90%. In the second experiment, we get precision of 95% and recall of 95%.

To evaluate spot detection, we compute F-measure scores on the binary maps supplied by the tested methods. Following [11], spot detection is stated as correct if the distance between the detected spot center and its corresponding ground truth center is less than four pixels. We report statistics on re-

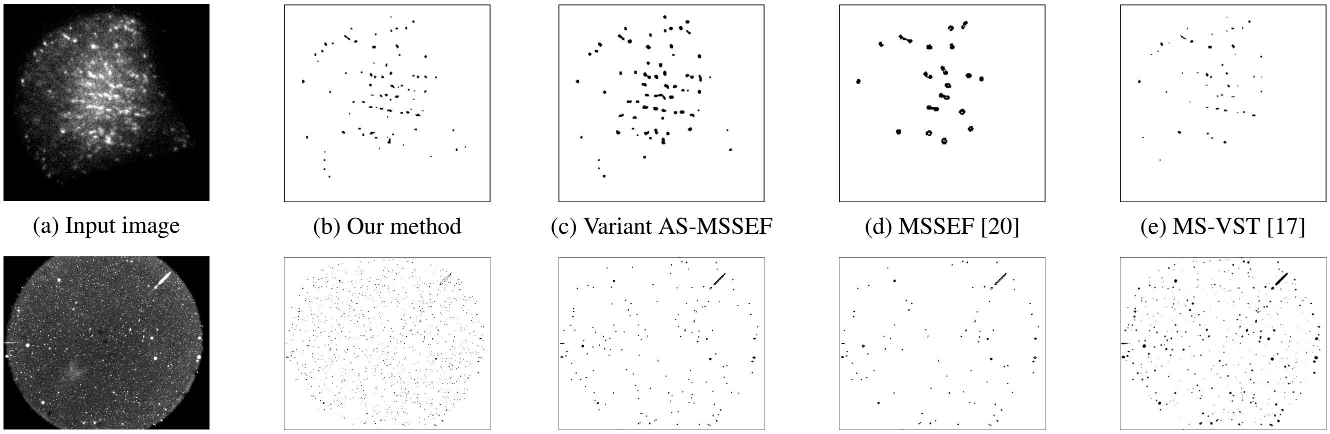

Fig. 1: Spots segmented (in black) by the four compared methods on a real TIRFM cell image (top row), and on a real astronomy image (bottom row). Images should be viewed (and zoomed in) in the pdf file for better visualization.

	Our method		AS-MSSEF		MSSEF		MS-VST	
	F-m.	Jacc.	F-m.	Jacc.	F-m.	Jacc.	F-m.	Jacc.
Mean	**0.982**	**0.724**	0.978	0.664	0.937	0.645	0.961	0.357
Std	**0.008**	0.052	0.009	0.068	0.037	0.048	0.015	**0.019**
Min	**0.966**	**0.641**	0.955	0.565	0.866	0.589	0.926	0.331
Max	**0.995**	**0.790**	**0.995**	0.745	0.989	0.708	0.989	0.386

Table 1: Statistics over the 40 simulated images of the two experiments on the F-measures and Jaccard index, obtained with the four compared methods

sults of the two experiments in Table 1. Let us point out that our method supplied the best F-measures for all the fourty images. For a few images, the variant AS-MSSEF yielded the same performance as our method, indicating that our multi-scale selection has a strong impact on the whole process.

Regarding spot segmentation assessment, we compute the overlap between the segmented spots in the binary map delivered by each method and the ground truth using the Jaccard index, defined as $J(A,B) = |A \cap B|/|A \cup B|$. As reported in Table 1, our method yields the best scores, meaning that our method better recovers size and shape of spots.

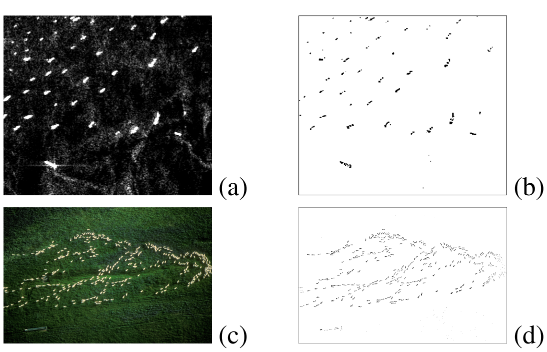

Fig. 2: Spots segmented (in black) by our method on a SAR satellite image including ships (top row) and an aerial color image depicting a sheep herd in a meadow (bottom row).

4.2. Real images

We have also carried out experiments on a set of diverse real images. Since there is no ground truth available, we rely only on visual assessment of spot segmentation, when comparing our method to others. For lack of space, we report two comparative experiments: on a total internal reflection fluorescence microscopy (TIRFM) cell image (by courtesy of Institut Curie) and on an astronomical image. Fig.1 contains the TIRFM input image (resp. astronomy image) and the maps of segmented spots obtained with our method, the variant AS-MSSEF, MSSEF and MS-VST. Our method selects 5 scales, $S^\star = \{1.728, 2.073, 2.488, 3.583, 6.191\}$, in the first real image (resp. 5 scales, $S^\star = \{1.440, 1.728, 5.159, 8.916, 15.407\}$, in the second one) as representative scales of the objects present in the image. Clearly, our method outperforms the three others, since we are closer to the right amount of objects to detect and are able to more accurately segment them. We also applied our single-scale method [3] to these images, and a subset of spots were missed. We report additional results in Fig.2, showing that our method can handle very different types of images with the same accuracy. It takes $1.25s$ to segment spots in a 500×500 image on a laptop with 2,8 GHz Intel Core i7 processor and 16 GB memory.

5. CONCLUSION

We have defined an original coarse-to-fine multi-scale spot detection method where we select multiple scales according to a criterion based on the *a contrario* approach. Experiments on simulated images with objective evaluation, and on real images with visual assessment, demonstrated that our method outperforms existing methods. Without introducing any critical parameter setting, our method is able to automatically select the relevant scales corresponding to spot-like objects of different sizes in the image, and to correctly segment spots, even in close proximity.

6. REFERENCES

[1] I. Smal, M. Loog, W. Niessen, and E. Meijering, Quantitative comparison of spot detection methods in fluorescence microscopy, *IEEE Trans. on Medical Imaging*, 29(2):282–301, Feb 2010.

[2] P. Ruusuvuori, Tarmo Äijö, S. Chowdhury, C. Garmendia-Torres, J. Selinummi, M. Birbaumer, A.M. Dudley, L. Pelkmans, and O. Yli-Harja, Evaluation of methods for detection of fluorescence labeled subcellular objects in microscope images, *BMC Bioinformatics*, 11(1):1–17, 2010.

[3] A. Basset, J. Boulanger, J. Salamero, P. Bouthemy, and C. Kervrann, Adaptive spot detection with optimal scale selection in fluorescence microscopy images, *IEEE Trans. on Image Processing*, 24(11):4512–4527, Nov. 2015.

[4] S. Ram, J.J. Rodrguez, and G. Bosco, Segmentation and detection of fluorescent 3D spots, *Cytometry Part A*, 81A(3):198–212, 2012.

[5] D. Sage, F. R. Neumann, F. Hediger, S. M. Gasser, and M. Unser, Automatic tracking of individual fluorescence particles: Application to the study of chromosome dynamics, *IEEE Trans. on Image Processing*, 14(9):1372–1383, Sep. 2005.

[6] D. Thomann, D. R. Rines, P. K. Sorger, and G. Danuser, Automatic fluorescent tag detection in 3D with super-resolution: Application to the analysis of chromosome movement, *Journal of Microscopy*, 208(1):49–64, 2002.

[7] K. Pan, A. Kokaram, J. Hillebrand, and M. Ramaswami, Gaussian mixture models for spots in microscopy using a new split/merge EM algorithm, In *IEEE Int. Conf. on Image Processing, ICIP'2010*, Sep. 2010.

[8] D. S. Bright and E. B. Steel, Two-dimensional top hat filter for extracting spots and spheres from digital images, *Journal of Microscopy*, 146(2):191–200, 1987.

[9] Pierre Soille, *Morphological image analysis: Principles and applications*, Springer-Verlag, 2nd edition, 2003.

[10] S. H. Rezatofighi, R. Hartley, and W. E. Hughes, A new approach for spot detection in total internal reflection fluorescence microscopy, In *9th IEEE Int. Symp. on Biomedical Imaging: From Nano to Macro, ISBI'2012*, May 2012.

[11] I. Smal, W. Niessen, and E. Meijering, A new detection scheme for multiple object tracking in fluorescence microscopy by joint probabilistic data association filtering, In *5th IEEE Int. Symp. on Biomedical Imaging: From Nano to Macro, ISBI'2008*, May 2008.

[12] L. Vincent, Morphological grayscale reconstruction in image analysis: Applications and efficient algorithms, *IEEE Trans. on Image Processing*, 2(2):176–201, Apr. 1993.

[13] T. Lindeberg, Scale-space for discrete signals, *IEEE Trans. on Pattern Analysis and Machine Intelligence*, 12(3):234–254, Mar. 1990.

[14] T. Lindeberg, Feature detection with automatic scale selection, *International Journal of Computer Vision*, 30(2):79–116, 1998.

[15] J. Piovano and T. Papadopoulo, Local statistic based region segmentation with automatic scale selection, In *European Conf. on Computer Vision, ECCV'2008*, Springer LNCS 5303, 2008.

[16] L. Gueguen and M. Pesaresi, Multi-scale Harris corner detector based on differential morphological decomposition, *Pattern Recognition Letters*, 32(14):1714–1719, 2011.

[17] B. Zhang, M. J. Fadili, J. L. Starck, and J.-C. Olivo-Marin, Multiscale variance-stabilizing transform for mixed Poisson-Gaussian processes and its applications in bioimaging, In *IEEE Int. Conf. on Image Processing, ICIP'2007*, Sep. 2007.

[18] J.-C. Olivo-Marin, Extraction of spots in biological images using multiscale products, *Pattern Recognition*, 35(9):1989 – 1996, 2002.

[19] H. Kong, H. C. Akakin, and S. E. Sarma, A generalized Laplacian of Gaussian filter for blob detection and its applications, *IEEE Trans. on Cybernetics*, 43(6):1719–1733, Dec 2013.

[20] A. Jaiswal, W. J. Godinez, R. Eils, M. J. Lehmann, and K. Rohr, Tracking virus particles in fluorescence microscopy images using multi-scale detection and multi-frame association, *IEEE Trans. on Image Processing*, 24(11):4122–4136, Nov. 2015.

[21] A. C. Jirapatnakul, S. V. Fotin, A. P. Reeves, A. M. Biancardi, D. F. Yankelevitz, and C. I. Henschke, Automated nodule location and size estimation using a multi-scale Laplacian of Gaussian filtering approach, In *31st Annual Int. Conf. of the IEEE EMBS, EMBC'2009*, Sep. 2009.

[22] A. Desolneux, L. Moisan, and J.-M. Morel, A grouping principle and four applications, *IEEE Trans. on Pattern Analysis and Machine Intelligence*, 25(4):508-513, Apr. 2003.

[23] T. Veit, F. Cao, and P. Bouthemy, An a contrario decision framework for region-based motion detection. *International Journal on Computer Vision*, 68(2):163-178, 2006.

[24] B. Grosjean and L. Moisan, A contrario detectability of spots in textured backgrounds, *Journal of Mathematical Imaging and Vision*, 33(3):313–337, Mar. 2009.